Comparison of CPTu and SDMT after 2012 Samara Earthquake, Costa Rica: liquefaction case studies

S. Amoroso
INGV Istituto Nazionale di Geofisica e Vulcanologia, L'Aquila, Italy

P. Monaco
University of L'Aquila, Italy

L.A. Vargas-Herrera & M. Coto-Loría
MYV Soluciones Geotécnicas, S.A, San José, Costa Rica

ABSTRACT: On September 5, 2012, a strong M_w = 7.6 earthquake hit Costa Rica. Its epicenter was located 10 km south of Samara, Guanacaste (offshore). This motion induced several geotechnical effects such as landslides, liquefaction, lateral spreading and local amplification. Of particular interest to the present paper was the occurrence of lateral spreading along several beaches located nearby the epicenter. The authors considered this a valuable opportunity to better understand this type of geotechnical phenomena. Contacts were made with the local governments in order to get access permits to two public beaches (Ostional and Garza). CPTu, SDMT, and disturbed sampling were carried out in order to gain an understanding of the geotechnical conditions that favored the occurrence of liquefaction. The aim of this paper is to use the latest methods for evaluating liquefaction potential based on SDMT and CPTu to back predict the observed phenomena and consequences. The main idea is to compare CPTu and SDMT as predictors of liquefaction for specific case studies.

1 INTRODUCTION

On September 5, 2012, a strong M_w = 7.6 earthquake hit Costa Rica. Its epicenter was located 10 km south of Samara, Guanacaste (offshore). Figure 1a shows a Google Earth image with the location of the epicenter (EP code) relative to the country. WGS84 coordinates of the epicenter were 9.777º and -5.569º and its depth was 14.2 km.

Several geotechnical dynamic phenomena were triggered by the earthquake and this is the reason the authors considered that this could be a good case study with plenty of information available for the study of complex phenomena such as liquefaction, whose occurrence was reported in several beaches nearby the epicenter (Costa Rica, Pacific North).

Contact with local authorities was successful and the authors gained access to those public beaches of interest in order to collect samples and perform in situ testing. Subsequently, the information was analyzed with published liquefaction methodologies in order to understand the observations.

A large accelerometer network managed by the LIS (Earthquake Engineering Laboratory) of the University of Costa Rica (UCR) allowed recording the earthquake in more than one hundred sites across Costa Rica. This information gave a lot of details regarding the distribution of the earthquake acceleration during the event. As an example, horizontal E-W PGA component is shown in contours through Costa Rica (see Figure 1b). As can be seen in Figure 1b, the larger PGAs were recorded nearby the epicenter with values close to 1500 gals. The higher PGAs were recorded in the Pacific North of Costa Rica, with values ranging between 500 gals and 1500 gals. The rest of the country experienced PGAs less than 500 gals. The latter explains why the most damage was concentrated in the Pacific North of Costa Rica.

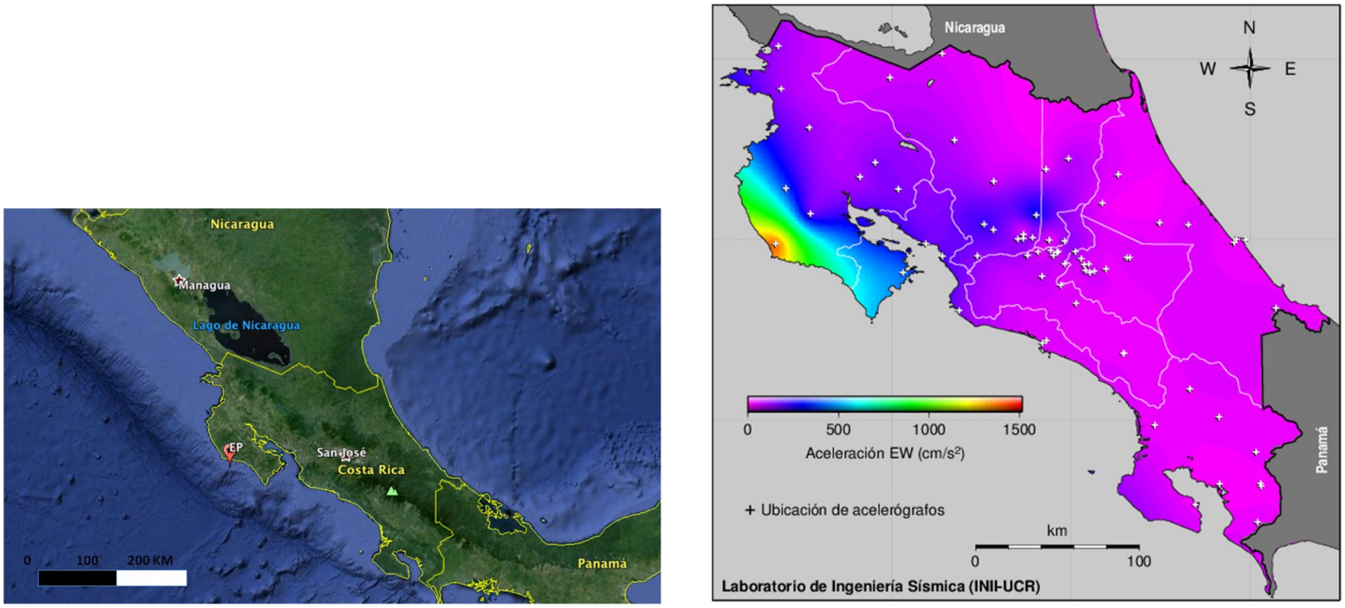

(a) (b)

Figure 1. (a) Location of the Earthquake Epicenter relative to the Region (EP = Epicenter) (Source: Google Earth). (b) Contours of E-W PGA across Costa Rica (Source: LIS, IINI-UCR 2013).

2 SELECTED SITES FOR RESEARCH

Given the amount and high quality of acceleration data available for the event, and also with the aid of the report prepared by a GEER team (GEER 2013), the authors decided to analyze the occurrence of liquefaction in two key beaches around the epicenter. The selected beaches were Ostional and Garza (Figure 2), where evidence of liquefaction on the surface was observed after the event, specifically lateral spreading. Transverse cracks, 1.50 meters in average, were observed in both beaches, approximately parallel to the shoreline (see Figure 2).

Figure 2. Location of Garza Beach and Ostional Beach relative to the epicenter.

Ostional and Garza are very close to an accelerometer station located in the city of Nosara, only 7-8 kilometers away from both sites. This accelerometer station belongs to the LIS–UCR network and for the purpose of this paper, it is called NOSARA. In Figure 2, the location of Nosara Station is shown in relation to the research sites (Ostional and Garza).

3 GEOLOGICAL CONTEXT AND PROPOSED SITE EXPLORATION

For the purpose of this paper, the geological setting for the sites of interest was determined and is shown in Figure 3. There is an important contrast between low lands (flat, composed of colluvium-alluvium deposits) and high lands (surrounding mountains, composed of basalts, sandstone, mudstone, and limestone). On the other hand, the geologic maps show a key geologic feature and that is the Abrasion Platform (dipping bedrock into the shore), which is key to understand the geotechnical findings.

The original exploration plan developed by the team included piezocone tests (CPTu), seismic dilatometer tests (SDMT, see Marchetti et al. 2008) and particle size analyses on samples. The testing program was the following: three pairs of SDMT-CPTu 20 m deep at Ostional Beach, three pairs of SDMT-CPTu 20 m deep at Garza Beach, one SDMT 30 m deep at Nosara Station, and disturbed (direct-push) sampling (Mostap) of the sand deposits at both beaches. The number of soundings and final depth of each were adjusted depending upon the real depth to bedrock (refusal). In Figure 3, the location of each point of interest is shown as follows: GZA-1, GZA-2, GZA-3 at Garza; OST-1, OST-2, OST-3 at Ostional and NOSARA ACC ST at Nosara. The description of the soundings is shown in Table 1, as well as indications of the depth of the Mostap samples and the fines content (*FC*) determined by sieve analysis on samples.

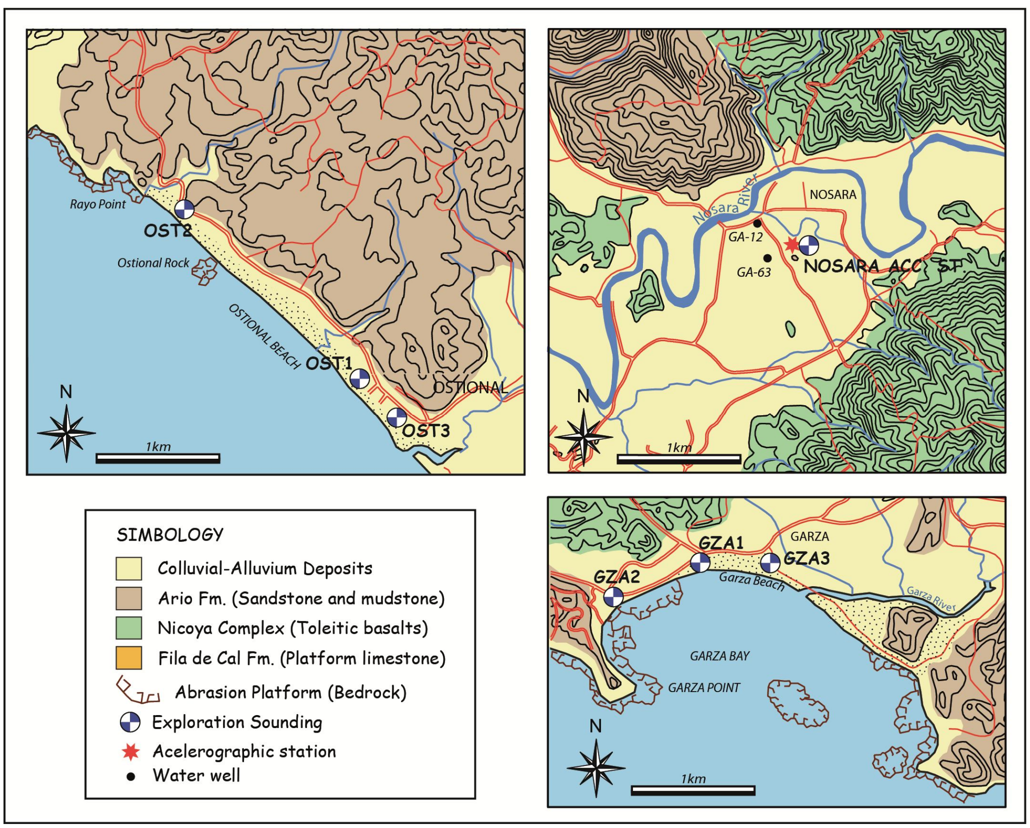

Figure 3. Geological setting for the sites of interest and proposed exploration plan. (Source: J.C. Duarte, MYV Team)

Table 1. Summary of the final exploration plan.

SITE	POINT OF INTEREST	CPTu Soundings	SDMT Soundings	MOSTAP Samples	FC (%)
OSTIONAL BEACH	OST-1	CPTu-1B (5.64 m), CPTu-1C (3.18 m)	SDMT-1A (3.00 m), SDMT-1B (5.80 m)	MS1 (3.0-3.6 m)	20.0
	OST-2	CPTu-2A (4.36 m), CPTu-2B (5.22 m)	SDMT-2 (5.00 m)	MS2 (3.4-4.8 m) and MS3 (1.5-2.8 m)	25.0 12.8
	OST-3	CPTu-3A (3.12 m), CPTu-3B (2.84 m), CPTu-3C (2.60 m)	SDTM-3A (1.80 m), SDMT-3B (2.80 m)	MS4 (2.0-3.0 m)	31.1
NOSARA ACC. ST.	NOSARA	---	SDMT-1 (8.00 m)	---	---
GARZA BEACH	GZA-1	CPTu-1A (3.68 m), CPTu-1B (3.66 m), CPTu-1C (3.88 m)	SDMT-1 (4.00 m)	MS5 (1.5-2.8 m)	10.0
	GZA-2	CPTu-2A (1.86 m), CPTu-2B (4.46 m), CPTu-2C (9.31 m)	SDMT-2 (6.20 m)	MS6 (5.8-7.2 m) and MS7 (1.0-2.2 m)	43.8 13.1
	GZA-3	CPTu-3A (15.11 m), CPTu-3B (16.53 m)	SDMT-3A (4.20 m), SDMT-3B (15.40 m)	MS8 (5.8-6.6 m) and MS9 (2.0-3.4 m)	17.0 13.0

Remark: Different subscripts (A, B, and C) represent different attempts to push either the cone or the DMT blade at the same location, when refusal was found. Between parentheses, the final depth of each sounding is shown.
SDMT = Seismic Dilatometer. CPTu = Piezocone. MS = Mostap Sample. FC = fines content from sieve analysis on samples.

4 CPTU AND SDMT TEST RESULTS

The results obtained from CPTu and SDMT are summarized in Figure 4 (Ostional Beach) and Figure 5 (Garza Beach). Figures 4a and 5a show the profiles with depth of the measured values (DMT pressure readings p_0 and p_1, CPTu corrected cone resistance q_t and sleeve friction f_s). Figures 4b and 5b show the profiles with depth of the normalized parameters, i.e. the material index I_D (indicating soil type) and the horizontal stress index K_D (related to stress history/OCR) obtained from SDMT, using common DMT interpretation formulae (Marchetti 1980, Marchetti et al. 2001), and the normalized cone resistance Q_{tn} and the soil behavior type index I_c obtained from CPTu, as well as the profile of the shear wave velocity V_S measured by SDMT. (To facilitate the comparison between results at the two test sites, the scale of the horizontal and vertical axes in Figures 4 and 5 is the same).

At both beaches the CPTu and SDMT results indicate the presence of shallow sand deposits, generally placed directly on the bedrock (in agreement with the geological setting shown in Figure 3), except at the location GZA-3, where the sand layer is placed on a silty clay layer. The ground water table is close to the ground surface (1.6 to 2 m depth at Ostional Beach, 1 m depth at Garza Beach).

5 LIQUEFACTION ANALYSIS

The liquefaction analysis was carried out according to the "simplified procedure" introduced by Seed & Idriss (1971), based on the comparison of the seismic demand on a soil layer generated by the earthquake (cyclic stress ratio *CSR*) and the capacity of the soil to resist liquefaction (cyclic resistance ratio *CRR*). If *CSR* is greater than *CRR*, liquefaction can occur.

For a preliminary assessment, the cyclic stress ratio *CSR* was estimated assuming two values of the peak ground acceleration *PGA* at the ground surface: (1) *PGA* = 1.4 g, i.e. equal to the *PGA* recorded at the Nosara Station, according to the shake maps developed by the LIS for the Sept 5, 2012 earthquake (Figure 1b, see also GEER 2013); (2) *PGA* = 0.44 g, corresponding to a design earthquake for a return period T_R = 475 years according to the Costa Rica Building Code 2010 (Zone IV, Site S_3). A magnitude scaling factor MSF = 0.974 was applied for the magnitude M_w = 7.6 Sept 5, 2012 main shock.

Future refinements will include the evaluation of CSR from site seismic response analysis, based on the ground motion recorded at the Nosara Station (where SDMT data are also available), combined with strong motion attenuation curves developed for the Costa Rica region. The sensitivity of the results to the assumed ground water level at the time of the earthquake will also be investigated.

The cyclic resistance ratio CRR was evaluated based on the results of adjacent CPTu and SDMT.

CRR from the CPTu was evaluated from the normalized clean sand cone resistance $Q_{tn,cs}$ using the method developed by Robertson & Wride (1998), in the form recommended by the 1996 NCEER and 1998 NCEER/NSF Workshops (Youd & Idriss 2001).

For the SDMT, two parallel independent estimates of CRR were obtained, at each depth, from the shear wave velocity V_S (measured) and from the horizontal stress index K_D (provided by current DMT interpretation).

CRR was evaluated from V_S using the correlation proposed by Andrus & Stokoe (2000).

Various CRR-K_D correlations have been developed in the last two decades, stimulated by the recognized sensitivity of K_D to a number of factors which are known to increase liquefaction resistance, such as stress history, prestraining/aging, cementation, structure, and by its correlation with relative density and state parameter (see e.g. Monaco et al. 2005). Four recent CRR-K_D correlations (Monaco et al. 2005, Tsai et al. 2009, Robertson 2012, Marchetti 2013) were used in this study. All four correlations were derived by translating current methods based on CPT (and SPT), supported by extensive case history databases, but using different approaches, e.g. using relative density as an intermediate parameter (Monaco et al. 2005) or direct correlations q_c -K_D established between the results of adjacent CPT-DMT tests (Tsai et al. 2009, Robertson 2012, Marchetti 2013).

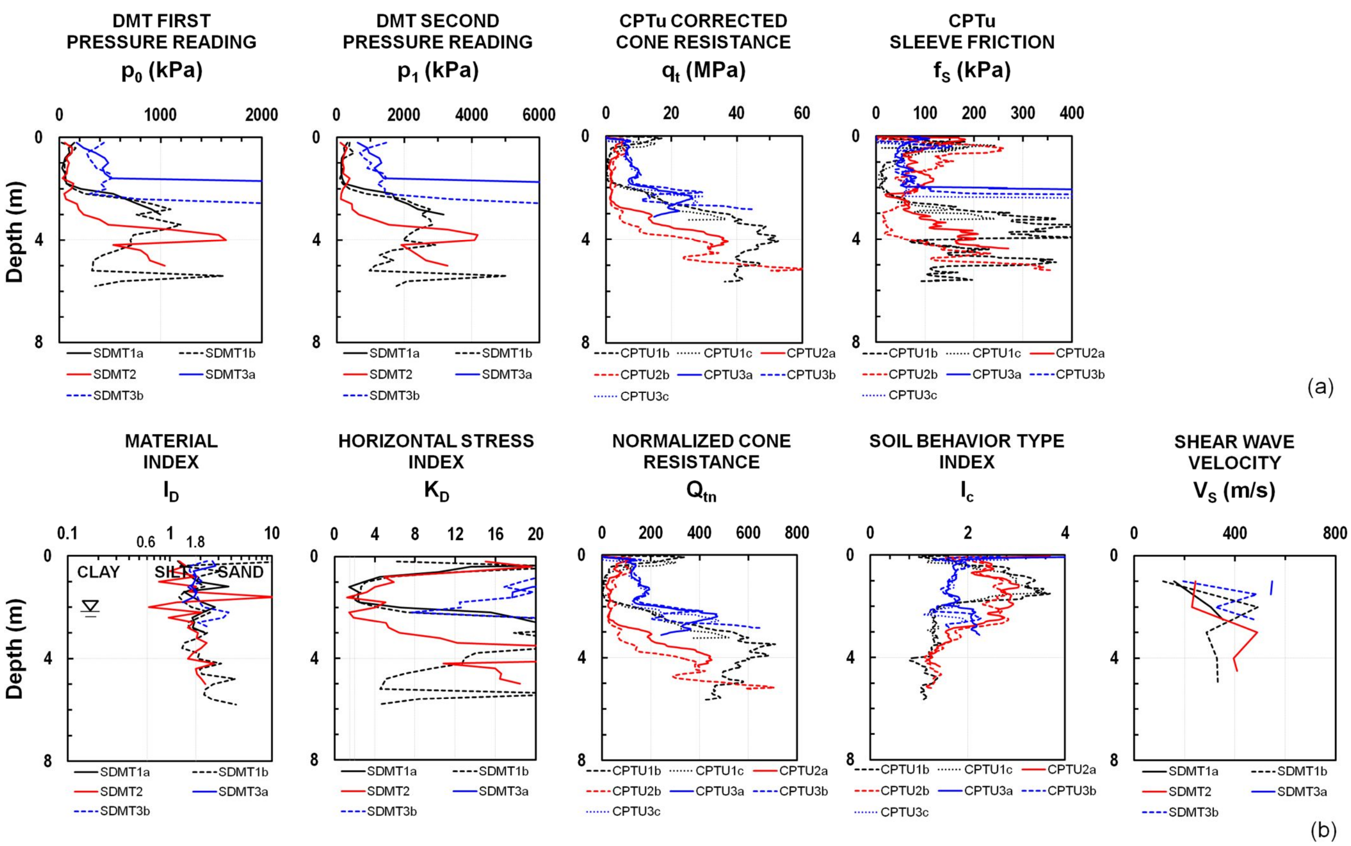

Figure 4. CPTu and SDMT results at Ostional Beach: (a) measured values, (b) normalized parameters and shear wave velocity.

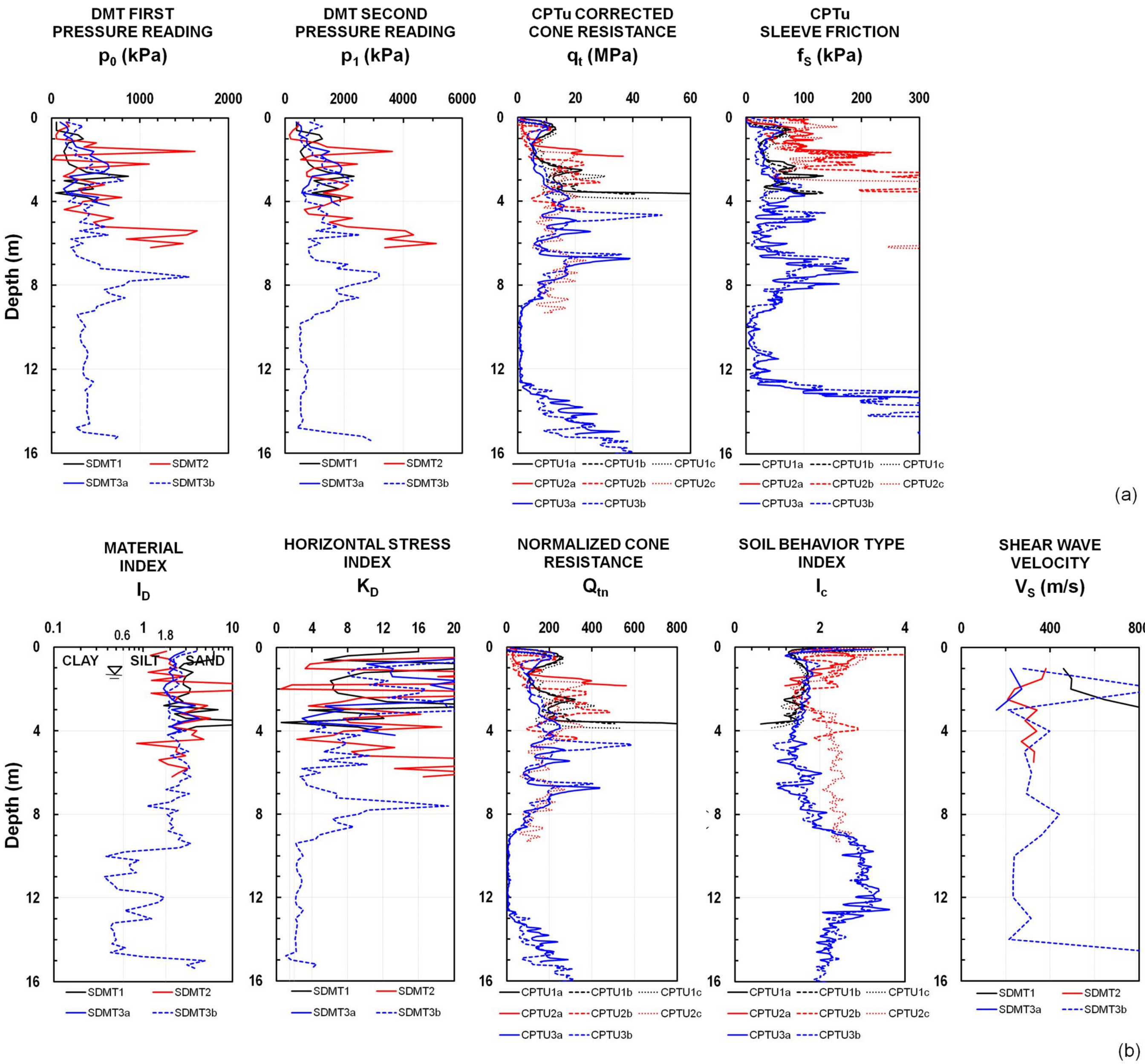

Figure 5. CPTu and SDMT results at Garza Beach: (a) measured values, (b) normalized parameters and shear wave velocity.

Some selected results of the analysis, obtained for the most severe seismic input condition (PGA = 1.4 g), are illustrated in Figure 6 (Ostional Beach) and Figure 7 (Garza Beach). Each diagram shows the profiles with depth of: (1) the soil behavior type index I_c (from CPTu) or the material index I_D (from SDMT); (2) the parameter used in each case for evaluating CRR: $Q_{tn,cs}$ (from CPTu), the shear wave velocity V_S or the horizontal stress index K_D (from SDMT); (3) the CSR, divided by the MSF, compared to the CRR; (4) the liquefaction safety factor $F_L = CRR_{M=7.5} / (CSR_{M=7.5} / MSF)$; (5) the liquefaction potential index I_L (Iwasaki et al. 1982), indicative of the overall liquefaction susceptibility of each site.

The most evident feature emerging from the comparison of the profiles of F_L and I_L obtained by different methods shown in Figures 6 and 7 is the substantial agreement between the predictions provided by methods based on the normalized cone resistance $Q_{tn,cs}$ (CPTu) and the horizontal stress index K_D (DMT). Both methods indicate that liquefaction occurred in the topmost sand layer, at local depths of ≈ 2-5 m below the ground surface at Ostional Beach (OST-1) and to ≈ 9 m depth, or below, at

Garza Beach (GZA-3). In the latter case the effects of liquefaction, globally expressed by the liquefaction potential index I_L, are particularly significant. In contrast, at both beaches no liquefaction was detected by the analysis based on the shear wave velocity V_S.

The same trend was observed in all other comparisons (not shown in this paper) at different test locations, both in Ostional Beach and Garza Beach.

It is also interesting to note that the analysis carried out assuming a much lower PGA = 0.44 g (design earthquake) provided similar results. In this case a moderate to high liquefaction hazard was pointed out at most test locations by both $Q_{tn,cs}$ and K_D (of course with I_L values lower than those calculated for PGA = 1.4 g), while V_S indicated no liquefaction hazard. All the above results point out a lower ability of V_S to detect liquefaction, compared with $Q_{tn,cs}$ and K_D.

It could be questioned that, since liquefaction generally occurred at shallow depths, the lower accuracy of CRR estimated by V_S may descend, at least in part, from the fact that downhole V_S methods tend to be less accurate at shallow depth. However, a similar discrepancy between CRR predicted by V_S and by K_D has been observed in several other cases investigated by SDMT (see e.g. Maugeri & Monaco 2006, Monaco & Marchetti 2007).

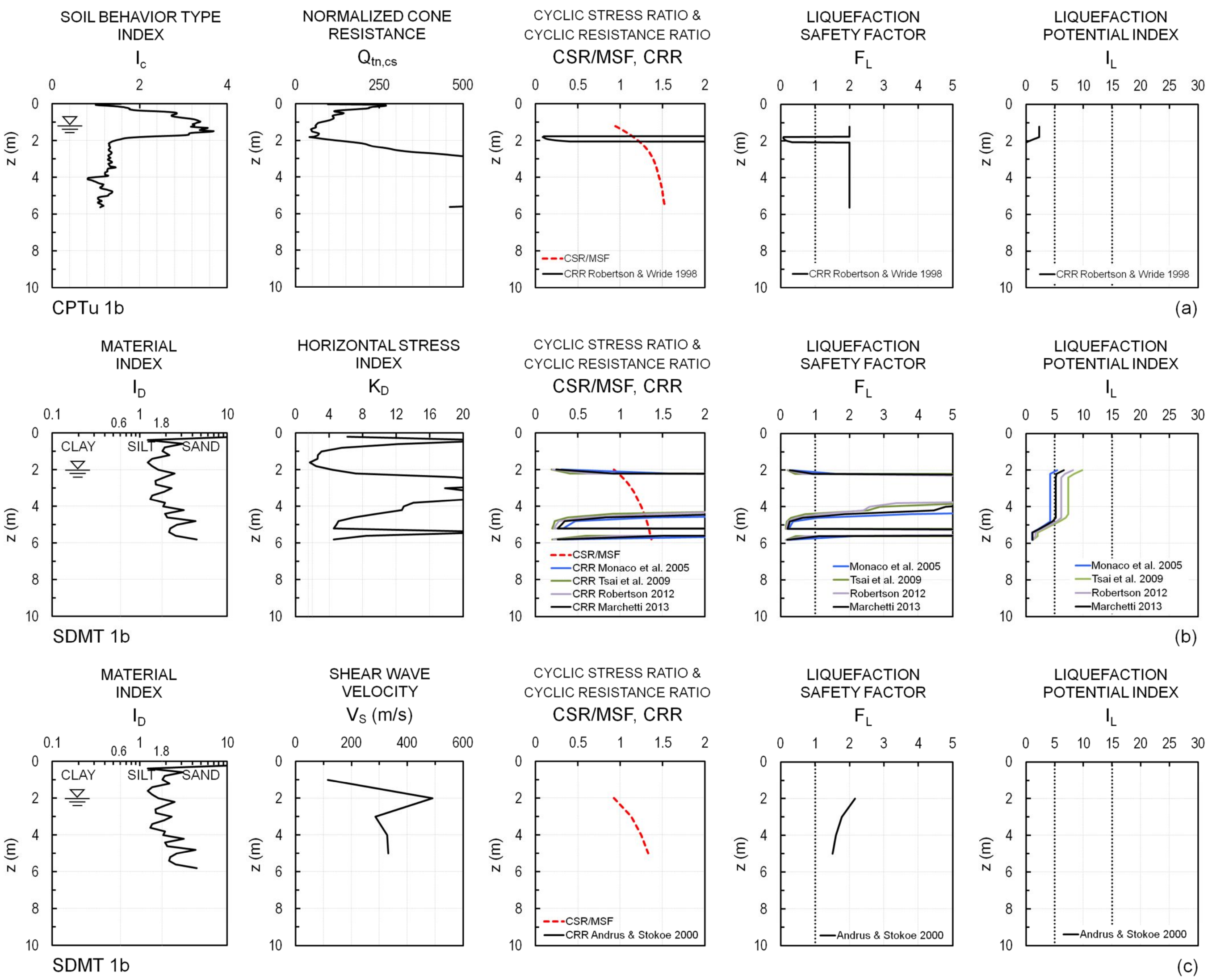

Figure 6. Ostional Beach, Site OST-1 (CPTu-1B, SDMT-1B) – Results of liquefaction analysis based on the normalized cone resistance $Q_{tn,cs}$ (a), the DMT horizontal stress index K_D (b) and the shear wave velocity V_S (c), for PGA = 1.4 g.

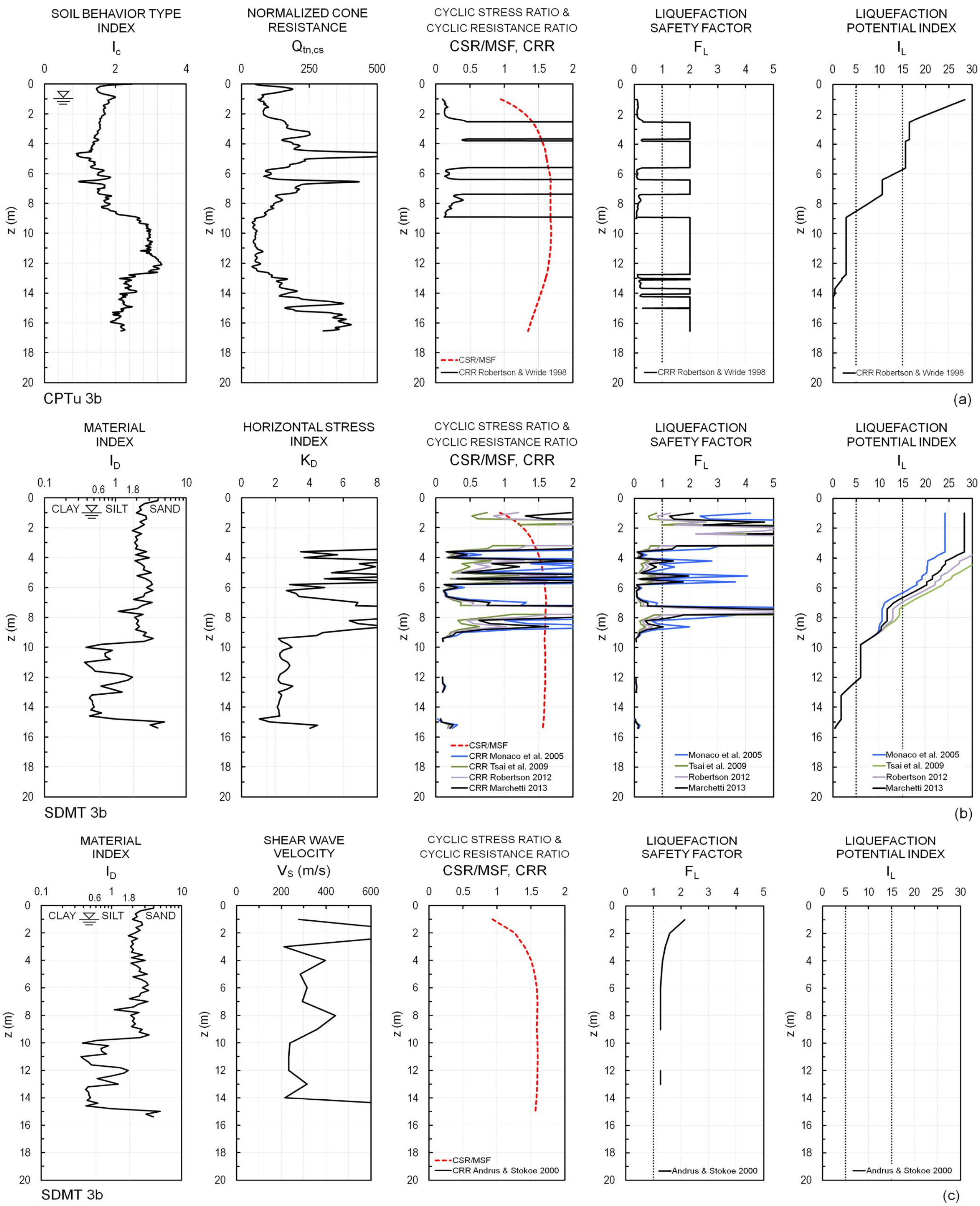

Figure 7. Garza Beach, Site GZA-3 (CPTu-3B, SDMT-3B) – Results of liquefaction analysis based on the normalized cone resistance $Q_{tn,cs}$ (a), the DMT horizontal stress index K_D (b) and the shear wave velocity V_S (c), for PGA = 1.4 g.

6 CONCLUSIONS

The liquefaction phenomena induced by the Sept 5, 2012 Samara earthquake were reproduced with reasonable accuracy by the analyses carried out using methods based on the normalized cone resistance $Q_{tn,cs}$ (CPTu) and the horizontal stress index K_D (DMT), according to the "simplified procedure". Both methods, generally in good agreement, indicate that liquefaction occurred in the topmost sand layer at various locations at Ostional Beach and at Garza Beach. In contrast, no liquefaction was detected by methods based on the shear wave velocity V_S, even for the most severe seismic input condition (PGA = 1.4 g). This finding points out a lower ability of V_S to detect liquefaction, compared with $Q_{tn,cs}$ and K_D.

The analyses illustrated in this paper indicate that the seismic dilatometer (SDMT) is a useful tool for assessment of the liquefaction hazard, confirming previous research work. This capability appears of great interest, since the use of "redundant" correlations, based on different in situ techniques/parameters, is generally recommended for a more reliable estimate of *CRR* (e.g. Robertson & Wride 1998, 1996-98 NCEER Workshops, Youd & Idriss 2001, and many others).

ACKNOWLEDGEMENTS

Julio Duarte (Geologist at MYV) and Diego Cordero (Geotech at MYV) are greatfully acknowledged.

REFERENCES

Andrus, R.D. & Stokoe, K.H., II. 2000. Liquefaction resistance of soils from shear-wave velocity. *J. Geotech. Geoenviron. Eng.*, ASCE, 126(11), 1015-1025.

GEER 2013. Geotechnical aspects of Sept. 5, 2012 M7.6 Samara, Costa Rica Earthquake. Version 1.0, Jan. 30, 2013.

Iwasaki, T., Tokida, K., Tatsuoka, F., Yasuda, S. & Sato, H. 1982. Microzonation for soil liquefaction potential using simplified methods. *Proc. 3rd Int. Conf. on Microzonation*, Seattle, 3, 1319-1330.

Marchetti, S. 1980. In Situ Tests by Flat Dilatometer. *J. Geotech. Engrg. Div.*, ASCE, 106(GT3), 299-321.

Marchetti, S. 2013. Personal communication.

Marchetti, S., Monaco, P., Totani, G. & Calabrese, M. 2001. The Flat Dilatometer Test (DMT) in Soil Investigations – A Report by the ISSMGE Committee TC16. *Proc. 2nd Int. Conf. on the Flat Dilatometer*, Washington D.C., 2006, 7-48.

Marchetti, S., Monaco, P., Totani, G. & Marchetti, D. 2008. In Situ Tests by Seismic Dilatometer (SDMT). In *From Research to Practice in Geotechnical Engineering*, *GSP No. 180*, ASCE, 292-311.

Maugeri, M. & Monaco, P. 2006. Liquefaction Potential Evaluation by SDMT. *Proc. 2nd Int. Conf. on the Flat Dilatometer*, Washington, D.C., 295-305.

Monaco, P. & Marchetti, S. 2007. Evaluating liquefaction potential by seismic dilatometer (SDMT) accounting for aging/stress history. *Proc. 4th Int. Conf. on Earthquake Geotechnical Engineering*, Thessaloniki, Greece, Paper 1626.

Monaco, P., Marchetti, S., Totani, G. & Calabrese, M. 2005. Sand liquefiability assessment by Flat Dilatometer Test (DMT). *Proc. XVI ICSMGE*, Osaka, 4, 2693-2697.

Robertson, P.K. 2012. The James K. Mitchell Lecture: Interpretation of in-situ tests – some insights. *Proc. 4th Int. Conf. on Geotechnical and Geophysical Site Characterization – ISC'4*, Porto de Galinhas, Brazil, 1, 3-24.

Robertson, P.K. & Wride, C.E. 1998. Evaluating cyclic liquefaction potential using the cone penetration test. *Canadian Geotech. J.*, 35(3), 442-459.

Seed, H.B. & Idriss, I.M. 1971. Simplified procedure for evaluating soil liquefaction potential. *J. Geotech. Engrg. Div.*, ASCE, 97(9), 1249–1273.

Tsai, P., Lee, D., Kung, G.T. & Juang, C.H. 2009. Simplified DMT-based methods for evaluating liquefaction resistance of soils. *Engineering Geology*, 103(2009), 13-22.

Youd, T.L. & Idriss, I.M. 2001. Liquefaction Resistance of Soils: Summary Report from the 1996 NCEER and 1998 NCEER/NSF Workshops on Evaluation of Liquefaction Resistance of Soils. *J. Geotech. Geoenviron. Eng.*, ASCE, 127(4), 297-313.